Available online at www.sciencedirect.com
SCIENCE DIRECT®
Electrochemistry Communications 5 (2003) 359–364
electrochemistry communications
www.elsevier.com/locate/elecom

Preparation of Mn-substituted $LiFeO_2$: A solid solution of $LiFeO_2$ and Li_xMnO_2

Y.S. Lee [a], S. Sato [b], Y.K. Sun [c], K. Kobayakawa [b], Y. Sato [b,*]

[a] *High-Tech Research Center, Kanagawa University, Yokohama 221-8686, Japan*
[b] *Department of Applied Chemistry, Kanagawa University, Yokohama 221-8686, Japan*
[c] *Department of Chemical Engineering, Hanyang University, Seoul 133-791, Republic of Korea*

Received 3 March 2003; received in revised form 12 March 2003; accepted 12 March 2003

Abstract

A new type of $LiFeO_2$–Li_xMnO_2 solid solution was synthesized at 350 °C under argon flow by a solid-state reaction. The doped Mn ions in the $LiMn_xFe_{1-x}O_2$ ($0 < x \leqslant 0.5$) obtained at 150 °C were regarded as an impurity in the orthorhombic $LiFeO_2$ structure and failed to form a perfect substitution form due to the low synthesis temperature. However, the $LiFeO_2$–Li_xMnO_2 solid solutions with various Mn contents (Mn/(Fe + Mn) = 0.1–0.5) were successfully obtained by calcination at 350 °C. Especially, the XRD pattern of the 50% Mn-substituted $LiFeO_2$ material was very similar to that of a lithiated Li_xMnO_2 compound. The Li/50% Mn-substituted $LiFeO_2$ cell exhibited not only a distinct increased voltage plateau in the 2.8 V region, but also an excellent cycling performance upto 50 cycles. We believe that this $LiFeO_2$–Li_xMnO_2 solid solution type compound has a unique electrochemical property in the cycling process.

Keywords: Orthorhombic $LiFeO_2$; Mn substituted; Solid solution; Cyclability

1. Introduction

Since Sony announced the commercial availability of their "lithium ion rechargeable battery" based on a carbon anode and a $LiCoO_2$ cathode in 1990, many research groups have tried many interactive improvements to the performance of lithium secondary batteries. In the case of cathode materials, layered $LiMO_2$ (M = Co, Ni, Mn, Fe) and spinel $LiMn_2O_4$ compounds were focused on due to their cost, thermal safety, and environmental aspects [1–6]. Among them, the $LiFeO_2$ compound is one of the best candidates from the viewpoint of cost because iron is the most abundant and cheapest metal in the world [7–15]. Recently, we reported that two kinds of $LiFeO_2$ materials, orthorhombic $LiFeO_2$ obtained at low temperature (150 °C) [16] and $Li_xFe_yO_z$ obtained at high temperature (800 °C) [17]. Furthermore, Kanno et al. also reported a new type of $LiFeO_2$ material with a tunnel structure, which showed a fairly good lithium insertion/extraction in the voltage range of 1.5–4.5 V [18]. However, many problems still remained; such as a lower operating voltage, no electrochemical activity (especially, the cubic α-, γ-form), and a poor (or low) cycle characteristic during the cycling test. This indication strongly prevented the use of $LiFeO_2$ as a practical cathode material, even though it has a significant merit based on cost.

In order to solve this problem, we tried to synthesize the $LiMn_xFe_{1-x}O_2$ ($0 \leqslant x \leqslant 0.5$) and Mn-substituted $LiFeO_2$ (Mn/(Fe + Mn) = 0.1–0.5) materials for improving the electrochemical characteristics of $LiFeO_2$ including the problem of the low operating voltage. Although some research groups have been investigating the role and meaning of the reaction of $Fe^{3+/4+}$ in the $LiCo_{1-x}Fe_xO_2$ and $LiNi_{1-x}Fe_xO_2$ systems, we believe that it is the first trial in which the cycling and electrochemical performances of $LiFeO_2$ system were improved by substituting Mn in this study, because previous studies were conducted on the $LiCoO_2$ and $LiNiO_2$ main systems. Furthermore, Tabuchi et al. recently reported

* Corresponding author. Tel./fax: +81-45-508-7480.
E-mail address: satouy01@kanagawa-u.ac.jp (Y. Sato).

1388-2481/03/$ - see front matter © 2003 Elsevier Science B.V. All rights reserved.
doi:10.1016/S1388-2481(03)00067-5

that the Fe-substituted Li_2MnO_3 (a type of solid solution) system as a 4 V cathode material [19]. They suggested that it showed a high possibility for use as a new cathode material in the 4 V region, because it presented a unique $Fe^{3+/4+}$ redox at 4 V and could form an electrochemically active phase of $LiFeO_2$ and Li_2MnO_3. We believe that this study was provided a good direction to cathode designers in synthesizing a new Fe-based cathode material. However, one different thing in this study versus the above report was that the orthorhombic $LiFeO_2$ material made by our group exhibited a fairly good cycle performance. Because they believed that the conventional and some layered $LiFeO_2$ materials, which were used in their study, are inactive and impossible to undergo insertion/extraction of lithium ions into the FeO_2 layers. It was the starting point to develop a new type of Fe-based material.

We report here the powder property and electrochemical characterization of a new type of Fe-based material, a solid-solution type of $LiFeO_2$ and Li_xMnO_2, which showed an excellent cycling performance at room temperature.

2. Experimental

Mn substituted $LiFeO_2$ ($0 \leqslant Mn/(Fe+Mn) \leqslant 0.5$) was synthesized using $LiOH \cdot H_2O$ (Kishida Chemical, Japan), γ-FeOOH (High Purity Chemicals, Japan), and γ-MnOOH (Tosoh Chemical, Japan) by a conventional solid-state method. A stoichiometric amount of each material was ground and calcined at 150 and 350 °C for 15 h in an argon atmosphere using a box furnace. The Li, Mn, and Fe contents in the resulting material were analyzed by atomic absorption spectroscopy (AA-6200, Shimadzu, Japan) by dissolving the powder in the dilute nitric acid.

The powder X-ray diffraction (XRD, Rint 1000, Rigaku, Japan) using CuKα radiation was used to identify the crystalline phase of the synthesized material. The particle morphology of the powder was observed using a scanning electron microscope (SEM, S-4000, Hitachi Co., Japan). The electrochemical characterizations were performed using a CR2032 coin-type cell. The cathode was fabricated with 20 mg of accurately weighed active material and 12 mg of conductive binder (8 mg of TAB and 4 mg of graphite). It was pressed on 200 mm^2 stainless steel mesh used as the current collector at a pressure of 300 kg/cm^2 and dried at 130 °C for 5 h in an oven. The test cell was made of a cathode and a lithium metal anode (Cyprus Foote Mineral Co.) separated by a porous polypropylene film (Celgard 3401). The electrolyte used was a mixture of 1 M $LiPF_6$–ethylene carbonate/dimethyl carbonate (1:2 by vol., Ube Chemicals, Japan). The charge and discharge current density was 0.4 mA/cm^2 with a cut-off voltage of 1.5–4.5 V at room temperature.

3. Results and discussion

In order to synthesize the $LiMn_xFe_{1-x}O_2$ ($0 \leqslant x \leqslant 0.5$) material, each starting material was thoroughly mixed and pressed at a 300 kg/cm^2 pressure into a 20 mm diameter pellet to improve the activity between the particles of the precursor. The synthetic method was the same as that for the synthesis of the orthorhombic $LiFeO_2$ material [16].

Fig. 1 shows the XRD patterns of the $LiMn_xFe_{1-x}O_2$ ($x = 0.0$, 0.1, 0.3, and 0.5) materials which were calcined at 150 °C for 15 h under flowing argon. The $LiFeO_2$ material obtained at 150 °C by a solid-state reaction has a well-developed orthorhombic phase in the XRD pattern (Fig. 1(a)). The lattice constants of this material are $a = 4.04$ Å, $b = 2.97$ Å, and $c = 6.07$ Å. However, other three $LiMn_xFe_{1-x}O_2$ materials exhibit quite different XRD patterns, although these maintained the main diffractions of the orthorhombic phase. Especially, the (0 0 1) peak at $2\theta = 14.6°$ slowly decreased compared with that of $LiFeO_2$ and it was split into the two parts upon Mn substitution. In the case of the $LiMn_{0.5}Fe_{0.5}O_2$ compound, it exhibited a very strong (1 0 1) peak and there are many impurities such as MnOOH. At first, we expected that the Mn ion (ionic radius of $Mn^{3+} = 0.72$ Å) could be easily substituted at the Fe (2*a*) site because it has a similar ionic radius compared to that of Fe^{3+} (0.69 Å) ion. However, we found no clear relation in the lattice constant as the Mn content increased, even though we ignored the existence of many impurities in the XRD pattern. Based on these results, it was considered that the $LiMn_xFe_{1-x}O_2$ ($x = 0.1$, 0.3, and 0.5) materials calcined at 150 °C seemed to fail to form a perfect substitution form, but just a type of mixture

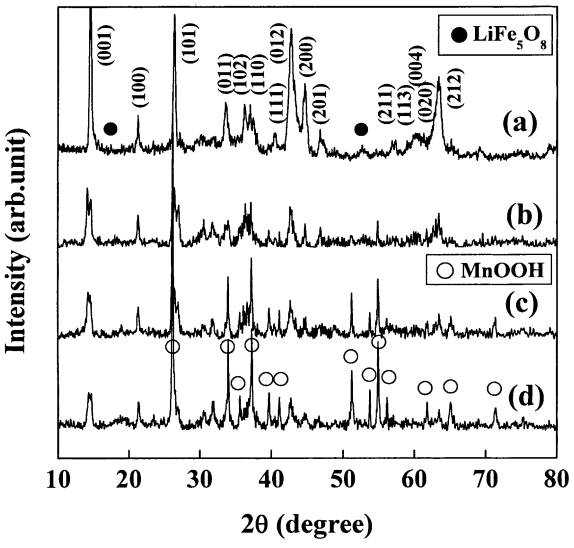

Fig. 1. XRD patterns of (a) $LiFeO_2$, (b) $LiMn_{0.1}Fe_{0.9}O_2$, (c) $LiMn_{0.3}Fe_{0.7}O_2$, and (d) $LiMn_{0.5}Fe_{0.5}O_2$. These materials were calcined at 150 °C for 15 h in argon.

between $LiFeO_2$ and γ-MnOOH. This indication could be explained from the thermal reaction in the γ-MnOOH material based on the calcination temperatures. It has already been reported a similar reaction system that $LiNO_3$ and γ-MnOOH mixtures can react at about 222–265 °C and it is transformed into the β-MnO_2 form in this range [20]. The endothermic reaction of this mixture suggested the following reaction.

$$LiNO_3(\text{solid}) + MnOOH(\text{solid}) \rightarrow Li_{0.3}MnO_2 + HNO_3 \quad (1)$$

It could form a lithiated $Li_{0.3}MnO_2$ material with an orthorhombic unit cell (Pnam) [20,21], which has a similar structure to the orthorhombic Li_xMnO_2 and $LiFeO_2$. Therefore, we could expect that a similar reaction might occur during the calcination process in this study, because it used similar starting materials. The thermogravimetric and differential thermal analyses of the precursor, which was LiOH, γ-FeOOH, and γ-MnOOH, are shown in Fig. 2. As expected, the precursor of the three starting materials presents two distinct endothermic peaks on the DTA curve. The first distinct peak around 80 °C is due to the removal of water from $LiOH \cdot H_2O$. The second peak at 221 °C shows the formation of β-MnO_2 as previously described. The transformation from γ-FeOOH to $LiFeO_2$ might slowly process until 150 °C, at which one could detect a small weight loss (a very slightly inclined plateau in the range of 100–150 °C) on the TGA curve. Conversely, it means that γ-MnOOH in the precursor was not involved in the synthetic reaction at a low calcination temperature (150 °C). It was confirmed that the remaining impurities in the XRD diagram and the amount (strength) of impurity peaks remarkably increased as the content of Mn ions increased. Therefore, we concluded that the material, which was obtained by using three starting materials at 150 °C should be considered not a type of $LiMn_xFe_{1-x}O_2$ compound, but a mixture of $LiFeO_2$ and MnO (or other Mn oxide form).

If added Mn ions are impurities in the $LiFeO_2$ structure at the lower temperature, is it possible to synthesize a different type of $LiMn_xFe_{1-x}O_2$ materials at higher (>150 °C) temperature? It was suspected that there is a high possibility to synthesize a new type of material over at 250 °C, which is shown to be a stable reaction step at about 300–350 °C. Fig. 3 shows the XRD patterns of the obtained materials at various Mn contents at 350 °C. Because the obtained materials at 350 °C are considered as different types of orthorhombic $LiFeO_2$ and $LiM_xFe_{1-x}O_2$ (M = transition metal), these materials are indicated as follows: a $LiFeO_2$–Li_xMnO_2 solid-solution type (10, 30, and 50% Mn-substituted $LiFeO_2$) compound. Various contents of the Mn-substituted $LiFeO_2$ materials showed different XRD patterns compared to those of $LiM_xFe_{1-x}O_2$ as shown in Fig. 1. There is no main (0 0 1) peak at $2\theta = 14.6°$ and the other major peaks were completely converted over whole scan range. Some of diffraction peaks, such as (0 2 0) and (0 2 1), increased as the substituted Mn content increased. Furthermore, the 50% Mn-substituted $LiFeO_2$ material had very similar to the XRD pattern as the Li_xMnO_2 material [22], although there remained still some small impurities. Based on these results, we considered that the obtained compounds in this study are the intermediate type of $LiFeO_2$–Li_xMnO_2 solid solutions.

Fig. 4 shows the SEM images of $LiFeO_2$ and the $LiFeO_2$–Li_xMnO_2 solid solution. As reported in a previous study [16], the $LiFeO_2$ powder consisted of 100–200

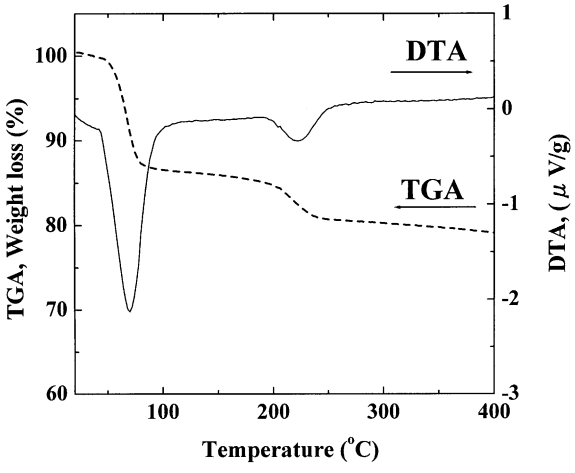

Fig. 2. Thermogravimetric and differential thermal analyses for precursor which was LiOH mixed with γ-MnOOH and γ-FeOOH. The mixture was dried in a vacuum oven at 25 °C prior to the thermal analyses and the heating rate was 5 °C/min under a N_2 atmosphere.

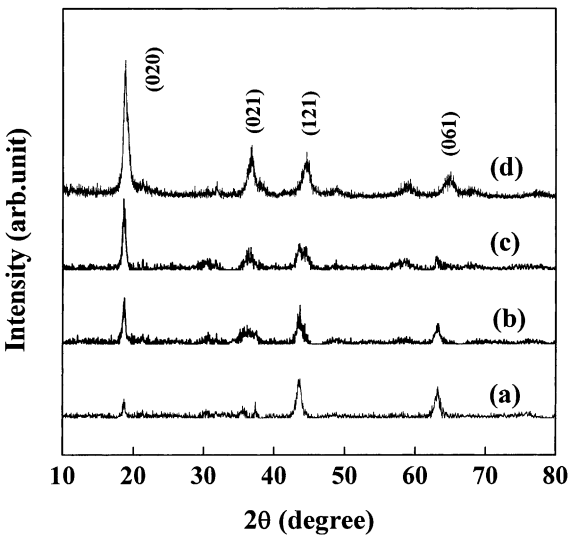

Fig. 3. XRD patterns of (a) 10%, (b) 30%, (c) 50% Mn-substituted $LiFeO_2$, and (d) Li_xMnO_2. These materials were calcined at 350 °C for 15 h in argon.

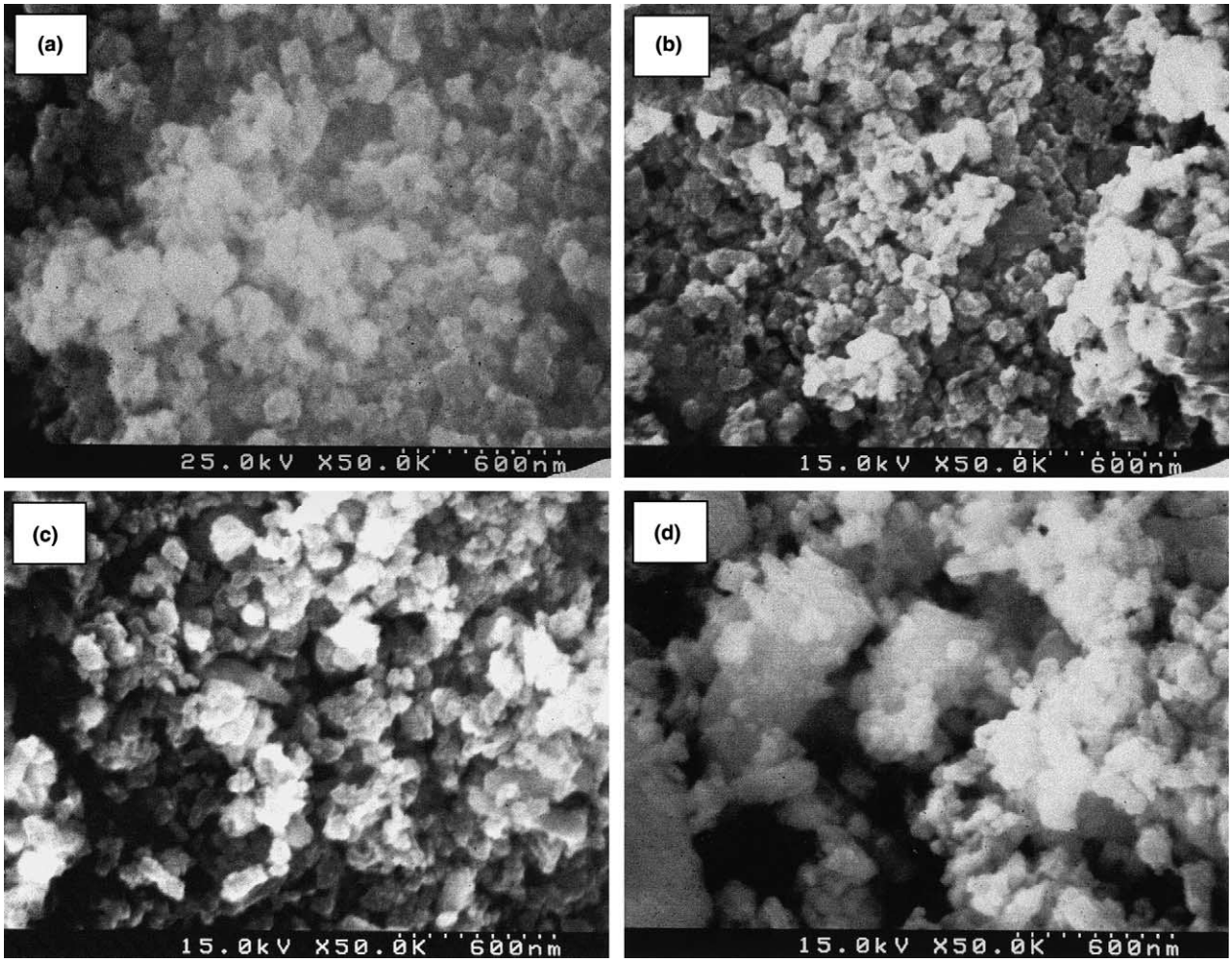

Fig. 4. Scanning electron micrographs of (a) $LiFeO_2$ (150 °C), (b) 10%, (c) 30%, and (d) 50% Mn-substituted $LiFeO_2$ powders obtained at 350 °C.

nm with needle-type particles. This is composed of an orthorhombic phase with a small amount of the β-$LiFe_5O_8$ ($a = 8.3$ Å) phase. Also, the 10% Mn-substituted $LiFeO_2$ material exhibits a similar particle size compared to that of the $LiFeO_2$ compound and has an evenly distributed particle shape over the whole range. However, the 30% Mn-substituted $LiFeO_2$ material shows a slightly increased particle size and the 50% Mn-substituted $LiFeO_2$ material has a remarkably changed particle shape/size. Some of the particles surprisingly increased to about 500–600 nm and other small particles at about 100–200 nm were distributed among the larger particles. It could be suspected that there might be induced a big difference in the powder properties between the 10% and 50% Mn-substituted $LiFeO_2$ materials, which is due to the remarkable increase in the particle size and shape during the calcinations process.

Fig. 5 shows the first charge/discharge curves of the Li/Mn-substituted $LiFeO_2$ (10, 30, and 50%) materials calcined at 350 °C in an argon atmosphere. The test condition was a current density of 0.4 mA/cm^2 between

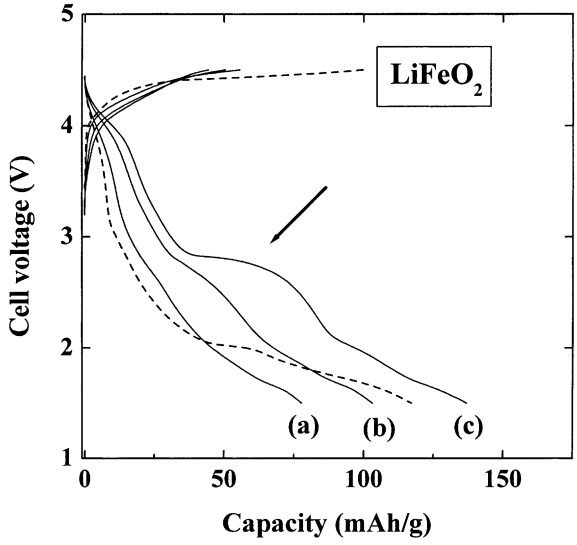

Fig. 5. The initial charge/discharge curves of (a) 10%, (b) 30%, and (c) 50% Mn-substituted $LiFeO_2$. The test conditions were a current density of 0.4 mA/cm^2 between 1.5 and 4.5 V at 25 °C.

4.5 and 1.5 V. Also presented in the first charge/discharge curve of the Li/$LiFeO_2$ cell (150 °C) in the same figure. As reported before [16], the Li/$LiFeO_2$ cell showed three voltage plateaus below 3.0 V in the discharge curve after showing an abrupt voltage drop at this point. Especially, the three distinct voltage plateaus are only displayed in the lower voltage region of 2.2–1.5 V, which is one of the main problems for using practical cathode materials for a lithium secondary battery. On the other hand, all the Li/Mn-substituted $LiFeO_2$ cells have quite different cycle behaviors, which are no distinct voltage in the lower voltage region, compared to that of the Li/$LiFeO_2$ cell. The Li/30% Mn-substituted $LiFeO_2$ cell starts to show a small change in the voltage profile at about 2.7 V and the discharge capacity after the first cycle increased from 78 (10% Mn-substituted) to 103 mA h/g. Furthermore, the Li/50% Mn-substituted $LiFeO_2$ cell shows not only a slightly changed voltage profile at 4.0 V, but also a clear voltage plateau at 2.8 V. We believe that the presence of the voltage plateau at 2.8 V results from the reduction reaction from Mn^{4+} to Mn^{3+} in the Li_xMnO_2 compound. More detailed electrochemical characterizations will be discussed in the technical paper.

Fig. 6 shows the variation in the specific discharge capacity with the number of cycles for the various Mn-substituted $LiFeO_2$ materials. The current density was 0.4 mA/cm^2 between 4.5 and 1.5 V. All the Li/Mn-substituted $LiFeO_2$ cells exhibited excellent cycling performances after 50 cycles and showed a significantly different capacity depending on the substituted Mn content. Although the 10% Mn-substituted $LiFeO_2$ presents a small initial discharge capacity of about 78 mA h/g and slightly decreased the cycle retention rate (<97.5%), the 50% Mn-substituted $LiFeO_2$ exhibited a high initial capacity of over 140 mA h/g and the discharge capacity increased until 50 cycles. The initial and last discharge capacities of this material are 137 and 158 mA h/g, respectively, with a charge/discharge efficiency of over 99% during the cycling test. It is noted that the discharge capacity of the 50% Mn-substituted $LiFeO_2$ after 50 cycles was two times higher than that of the 10% Mn-substituted $LiFeO_2$. This means that the substituted Mn ions easily formed a solid solution with $LiFeO_2$ at the increased calcination temperature (350 °C) and play a role in the increased reversible discharge capacity, which occurred for the $Mn^{4+/3+}$ redox reaction in the 2.8 V region.

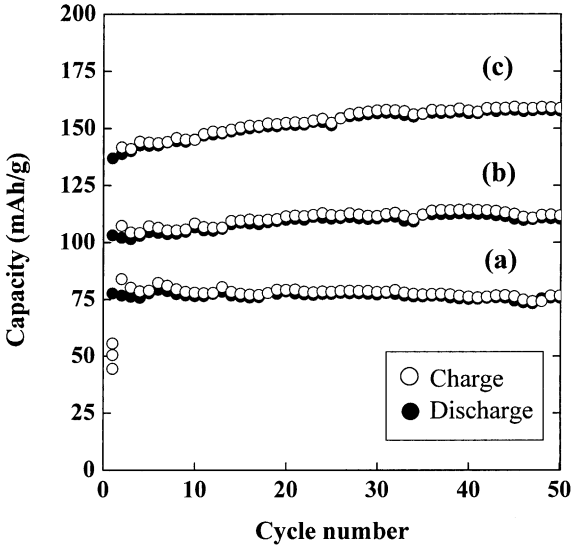

Fig. 6. Specific discharge capacity versus cycle number for Li/Mn-substituted $LiFeO_2$ cells. (a) 10%, (b) 30%, and (c) 50% Mn-substituted $LiFeO_2$. The test conditions were a current density of 0.4 mA/cm^2 between 1.5 and 4.5 V at 25 °C.

4. Conclusion

A new type of $LiFeO_2$–Li_xMnO_2 solid solution was synthesized at 350 °C under argon flow by a solid-state reaction. The XRD pattern of the 50% Mn-substituted $LiFeO_2$ material was very close to that of Li_xMnO_2 compound. It was composed many large particles of about 500–600 nm and small particles of about 100–200 nm, which were distributed among the larger particles. Especially, the Li/50% Mn-substituted $LiFeO_2$ cell exhibited not only a distinct voltage plateau in the 2.8 V region, but also an excellent cycling performance upto 50 cycles. It was considered that this unique voltage plateau resulted from the redox reaction from Mn^{4+} to Mn^{3+} in the 3 V region. We believe that $LiFeO_2$–Li_xMnO_2 solid solution could be a new type of cathode material by optimizing the substituted Mn content.

Acknowledgements

The authors gratefully acknowledge the financial support by the High-Tech Research Center Project from the Ministry of Education, Culture, Sports, Science and Technology.

References

[1] K. Mizushima, P.C. Jones, P.J. Wiseman, J.B. Goodenough, Mater. Res. Bull. 15 (1980) 783.
[2] J.R. Dahn, U. Von Sacken, C.A. Michel, Solid State Ionics 44 (1990) 87.
[3] T. Ohzuku, A. Ueda, M. Nagayama, J. Electrochem. Soc. 140 (1993) 1862.
[4] H. Arai, S. Okada, Y. Sakurai, J. Yamaki, Solid State Ionics 95 (1997) 275.
[5] L. Croguennec, P. Deniard, R. Brec, A. Lecerf, J. Mater. Chem. 5 (1995) 1919.
[6] Y.I. Jang, B. Huang, H. Wang, D.R. Sadoway, Y.M. Chiang, J. Electrochem. Soc. 146 (1999) 3217.

[7] R. Kanno, T. Shirane, Y. Kawamoto, Y. Takeda, M. Takano, M. Ohashi, Y. Yamaguchi, J. Electrochem. Soc. 146 (1996) 2435.
[8] T. Shirane, R. Kanno, Y. Kawamoto, Y. Takeda, M. Takano, T. Kamiyama, F. Izumi, Solid State Ionics 79 (1995) 227.
[9] M. Tabuchi, K. Ado, H. Sakaebe, C. Masquelier, H. Kageyama, O. Nakamura, Solid State Ionics 79 (1995) 220.
[10] M. Tabuchi, C. Masquelier, T. Takeuchi, K. Ado, I. Matsubara, T. Shirane, R. Kanno, S. Tsutsui, S. Nasu, H. Sakaebe, O. Nakamura, Solid State Ionics 90 (1996) 129.
[11] K. Ado, M. Tabuchi, H. Kobayashi, H. Kageyama, O. Nakamura, Y. Inaba, R. Kanno, M. Takagi, Y. Takeda, J. Electrochem. Soc. 144 (1997) L177.
[12] M. Tabuchi, S. Tsutsui, C. Masquelier, R. Kanno, K. Ado, I. Matsubara, S. Nasu, H. Kageyama, J. Solid State Chem. 140 (1998) 159.
[13] M. Tabuchi, K. Ado, H. Kobayashi, I. Matsubara, H. Kageyama, M. Wakita, S. Tsutsui, S. Nasu, Y. Takeda, C. Masqulier, A. Hirano, R. Kanno, J. Solid State Chem. 141 (1998) 554.
[14] Y. Sakurai, H. Arai, S. Okada, J. Yamaki, J. Power Sources 68 (1997) 711.
[15] Y. Sakurai, H. Arai, J. Yamaki, Solid State Ionics 113–115 (1998) 29.
[16] Y.S. Lee, C.S. Yoon, Y.K. Sun, K. Kobayakawa, Y. Sato, Electrochem. Commun. 4 (2002) 727.
[17] Y.T. Lee, Y.S. Lee, Y. Sato, Y.K. Sun, Electrochem. Commun., submitted for publication.
[18] T. Matsumura, R. Kanno, Y. Inaba, Y. Kawamoto, M. Takano, J. Electrochem. Soc. 149 (2002) L1509.
[19] M. Tabuchi, A. Nakashima, H. Shigemura, K. Ado, H. Kobayashi, H. Sakaebe, H. Kagayama, T. Nakamura, M. Kohzaki, A. Hirano, R. Kanno, J. Electrochem. Soc. 149 (2002) A509.
[20] Y. Xia, M. Yoshio, J. Power Sources 57 (1995) 125.
[21] M.M. Thackeray, M.H. Rossouw, R.J. Gummow, D.C. Liles, K. Pearce, A. De Kock, W.I.F. Davis, S. Hull, Electrochim. Acta 38 (1993) 1259.
[22] H. Nakamura, K. Motooka, H. Noguchi, M. Yoshio, J. Power Sources 81–82 (1999) 632.